

## A respiration–diffusion model for ‘Conference’ pears II. Simulations and relation to core breakdown

J. Lammertyn<sup>a,\*</sup>, N. Scheerlinck<sup>a</sup>, P. Jancsó<sup>b</sup>, B.E. Verlinden<sup>a</sup>,  
B.M. Nicolaï<sup>a</sup>

<sup>a</sup> Department of Agro Engineering and –Economics, Flanders Centre/Laboratory of Postharvest Technology, Catholic University Leuven, B-3001 Leuven, Belgium

<sup>b</sup> Department of Agro Engineering and –Economics, Laboratory of Agro-Machinery and Processing, Catholic University Leuven, Leuven, Belgium

Received 14 August 2002; accepted 23 March 2003

### Abstract

A respiration–diffusion model for ‘Conference’ pears was used to simulate three-dimensional internal O<sub>2</sub> and CO<sub>2</sub> concentration profiles for intact pears as a function of the storage conditions. Although the skin was the major barrier to gas transport, the internal gas gradients in the fruit could not be neglected. Especially at high temperatures, when the respiration rate is high, the internal gradients increased considerably. A sensitivity analysis was carried out to assess the effect of biological variability present on the respiration and diffusion parameters, and on the gas concentration profiles. It was found that at room temperature, the O<sub>2</sub> concentration underneath the fruit skin is mainly determined by the O<sub>2</sub> transfer coefficient and consumption rate. However, for typical storage temperatures this dependency is less pronounced. A comparison of simulated gas concentration contours of pears stored with delayed controlled atmosphere and those immediately stored under controlled atmosphere (CA), illustrated the importance of an appropriate storage management right after harvest. When CA storage was applied immediately after harvest, the O<sub>2</sub> and CO<sub>2</sub> concentrations reached very low and very high values, respectively, possibly causing irreversible membrane damage and inducing core breakdown. These values were not found for delayed controlled atmosphere. A model validation experiment on affected pears indicated that the diffusion and respiration parameters for affected tissue were different from those for healthy tissue.

© 2003 Elsevier B.V. All rights reserved.

**Keywords:** Controlled atmosphere; Modelling; *Pyrus communis* L.; Respiration–diffusion

### 1. Introduction

Controlled atmosphere storage has proven to be beneficial for long-term storage of pears. A reduced O<sub>2</sub> concentration and a slightly increased CO<sub>2</sub> concentration in combination with a low

\* Corresponding author. Tel.: +32-16-32-23-76; fax: +32-16-32-29-55.

E-mail address: [jeroen.lammertyn@agr.kuleuven.ac.be](mailto:jeroen.lammertyn@agr.kuleuven.ac.be) (J. Lammertyn).

temperature slow down the ripening processes. However, sub-optimal or too severe controlled atmosphere conditions can cause irreversible changes in the fruit metabolism resulting in internal storage disorders such as core breakdown in ‘Conference’ pears, which is characterised by brown discoloration of the tissue around the core and the development of cavities. None of these symptoms can be observed from the outside. Wang and Wang (1989) and Lammertyn et al. (2003a) studied the process of core breakdown in pears non-destructively by means of magnetic resonance imaging and X-ray computer tomography. They found that the contours of the brown discoloured tissue were parallel to the fruit boundaries, suggesting a relation between tissue and skin gas diffusion properties and the disorder. Since gas exchange of the fruit with the environment consists of both respiration and gas diffusion, a respiration–diffusion model may, therefore, be the most appropriate to study the local internal gas concentrations in the fruit and their relation to the disorder symptoms. Models describing gas diffusion and respiration have been reported in literature, e.g. apples (Mannapperuma et al., 1991; Rabus et al., 2001) and potato tubers (Abdul-Baki and Solomos, 1994). A respiration–diffusion model for ‘Conference’ pears has been constructed and validated successfully by Lammertyn et al. (2003b). With this respiration–diffusion model, it is possible to evaluate the effect of arbitrary storage conditions on the internal local gas concentrations and to relate these gas profiles to the occurrence of core breakdown symptoms.

The objective of this paper consists of three parts. First, the constructed respiration–diffusion model will be used to calculate the local internal gas concentration profiles in the pear as a function of different storage atmospheres and temperatures. Second, a sensitivity analysis will be carried out to investigate the influence of skin and tissue gas diffusion or respiration parameters on the internal local gas concentrations in the fruit. Finally, the respiration–diffusion model will be applied to study the relation between internal gas profiles and core breakdown disorder symptoms. In this context, the constructed reaction–diffusion

model (Lammertyn et al., 2003b) will be evaluated for pears already affected by the disorder.

## 2. Materials and methods

### 2.1. Simulations

With the respiration–diffusion model, steady-state  $O_2$  and  $CO_2$  concentration profiles at different storage atmospheres (Table 1) were simulated for intact pears using the method of Lammertyn et al. (2003b). To study the temperature effect on the gas distribution in the pear, simulations were carried out for a pear stored in air at  $-1$ ,  $7$  and  $20$  °C. The effect of  $CO_2$  concentration (0.7 or 5%) under ultra-low  $O_2$  storage was deduced from two simulations at 2%  $O_2$  and  $-1$  °C, and the influence of the presence of a cavity on the gas concentration contours was studied under shelf life conditions.

### 2.2. Sensitivity analysis

Due to biological variability, the model parameters determined from independent experiments are subject to variation. To assess the effect of this variation on the model results, a sensitivity analysis was carried out. Such an analysis studies how sensitive a particular predicted model value (e.g. the  $O_2$  concentration in a pear cavity) is with regard to small changes in model parameters. The relative sensitivities were calculated as normalised partial derivatives of gas concentration,  $G$ , with respect to the model parameters,  $P_i$ .  $G$  denotes the

Table 1  
Storage conditions for which respiration–diffusion model simulations were carried out

| Storage description      | $T$ (°C) | $O_2$ (%) | $CO_2$ (%) |
|--------------------------|----------|-----------|------------|
| Shelf life               | 20       | 20.8      | 0          |
| Refrigerator             | 7        | 20.8      | 0          |
| Precooling               | $-1$     | 20.8      | 0          |
| Disorder inducing        | $-1$     | 2         | 5          |
| Optimal CA               | $-1$     | 2         | 0.7        |
| Shelf life (with cavity) | 20       | 20.8      | 0          |

O<sub>2</sub> or CO<sub>2</sub> concentration and  $P_i$  stands for every respiration–diffusion model parameter listed in Table 1 of Lammertyn et al. (2003b). For example, to calculate the relative sensitivity of the gas concentration,  $G$ , with respect to parameter  $P_i$ , the following formula was used:

$$J_{G,P_i}^r = \frac{\partial G/G}{\partial P_i/P_i} \cong \frac{G_{P_i+\Delta P_i} - G_{P_i-\Delta P_i}}{2\Delta P_i} \frac{P_i}{G} \quad (1)$$

with  $\Delta P_i$  a small perturbation, here taken as 1% of the nominal value of  $P_i$  which was used for the estimation. The relative sensitivity denotes the relative change of the estimated value of  $G$  corresponding to a relative change of the model parameter. A comparison of the relative sensitivities between the different parameters indicates which model parameters most severely influence the model prediction results (Nicolai et al., 2000).

A sensitivity analysis of the respiration model simulations was carried out for two situations, corresponding to the experiments used to validate the respiration–diffusion model as described in Lammertyn et al. (2003b). A first sensitivity analysis was performed on the O<sub>2</sub> consumption and CO<sub>2</sub> production rates (or fluxes) of an intact pear simulated with the respiration–diffusion model. Since the sensitivity analysis depends on the ambient gas atmosphere for which the respiration rates are simulated, it was carried out for three gas atmospheres at 20 °C: 20.8% O<sub>2</sub>+0% CO<sub>2</sub>, 8% O<sub>2</sub>+15% CO<sub>2</sub> and 1% O<sub>2</sub>+0% CO<sub>2</sub>. In a second sensitivity analysis, the effect of small changes in respiration and diffusion parameters on the O<sub>2</sub> and CO<sub>2</sub> concentrations underneath the skin was evaluated. This was repeated for three storage conditions: 20.8% O<sub>2</sub>+0% CO<sub>2</sub> at 20 °C, 20.8% O<sub>2</sub>+0% CO<sub>2</sub> at 1 °C and 0% O<sub>2</sub>+0% CO<sub>2</sub> at 20 °C.

### 2.3. Respiration–diffusion model in relation to core breakdown

#### 2.3.1. Fruit material

Pears were harvested in a commercial orchard in Zellik (Belgium) on the 25th of September 2000, 10 days after the commercial harvest date. Twenty pears were cooled for 7 days at 1 °C in air and

subsequently stored for 9 months in core breakdown disorder-inducing conditions (1 °C, 10% CO<sub>2</sub> and 1% O<sub>2</sub>) (Lammertyn et al., 2000). After removal fruit were imaged with X-ray CT to non-destructively detect internal browning and cavities.

#### 2.3.2. X-ray CT measurements

The X-ray CT scans were made on a tomography system (Microfocus Computer Tomography, AEA, Tomohawk, Philips, The Netherlands) using an X-ray source (Philips HOMX 161) operated at 53 kV and 0.21 mA. The exiting radiation was detected by a CCD camera (JAI M50). A HOMX161 object manipulator was used to position the detector and the object table. A stepper motor (Servostep 1700) was used to rotate and move the pear during the X-ray CT measurement to suppress CT image ring artefacts. The pear was positioned in a plastic cylindrical support device. Software (Tomohawk version 3.5.2, AEA Technology, UK) was used to reconstruct the CT scans from the X-ray transmission data.

#### 2.3.3. Gas atmosphere composition in cavity

To evaluate the validity of the respiration–diffusion model on affected pears, it was chosen to exploit the presence of the cavities in the disordered pears. Twenty pears were stored under disorder-inducing conditions. Based on two-dimensional X-ray projection images, the three pears with the largest internal cavities were selected for a further tomographic analysis with X-ray CT. Fifty X-ray CT scans were taken of each pear, applying the equipment settings described in Section 2.3.2. A computer vision system developed by Jancsó (1999) was used to reconstruct the volume of the (intact) pears (Lammertyn et al., 2003b). The cavities were included based on X-ray CT scans as will be described in Section 2.3.4. The resulting finite element meshes of the three pears with cavities were used for simulation purposes. Simulations of the steady-state internal O<sub>2</sub> and CO<sub>2</sub> concentrations were carried out at the same atmospheric conditions and temperatures as for the real experiments.

The three pears were put in 1.8 l glass jars and stored at three different storage conditions, in order to cover the whole model range. A first pear

was stored at 100% N<sub>2</sub> and 20 °C. The aim of this experiment was to validate the fermentative metabolism of the fruit. The second pear was stored at 21% O<sub>2</sub>, 0% CO<sub>2</sub> at 20 °C. This experiment validates both the O<sub>2</sub> consumption and the CO<sub>2</sub> production rate of the fruit. For the third pear, the same storage conditions as for the previous one were taken but the temperature was decreased to 1 °C. In this experiment, used to validate the temperature effect on the gas exchange of the fruit, it was assumed that neither the Michaelis-Menten constants nor the gas diffusion properties were temperature-dependent. The former assumption is acceptable (Hertog et al., 1998); however, the latter might be questionable (Yearsley et al., 1997). The gas mixtures were made with a gas mixing panel and humidified to prevent drying of the pears. The flow rate was equal to 10 l h<sup>-1</sup>. The pears were equilibrated in their respective atmosphere for 60 h. A hypodermic needle was adapted in order to prevent blocking at the tip while inserting it in the pear cavity. The tip was filled with wax and a slit was made in the needle shaft parallel to the tip at 5 mm of it. Based on the 50 X-ray CT scans, the exact position to put the needle was determined and a septum was glued at that position of the pear surface in order to prevent gas exchange between the cavity and the ambient atmosphere during the measurements; a small movement of the needle could otherwise create an air channel to the environment. A sample of 1 ml was taken and analysed with a micro-GC (Chrompack CP 2002, The Netherlands).

#### 2.3.4. *Reconstruction of cavity in pear with X-ray CT*

To simulate the gas concentrations in pear cavities, three-dimensional finite element meshes of pears with cavities needed to be constructed. The finite element meshes were based on shape measurements of real fruits with cavities. X-ray CT scans of these pears (Fig. 1A) were taken as described previously. The contour lines of the cavities were extracted from all X-ray CT scans using the MATLAB Image Processing toolbox (Jancsó et al., 2001) and a three-dimensional geometrical model of the cavity was reconstructed.

For the three-dimensional model generation, first periodic (closed) spline curves were fitted to the cavity contour lines and then the splines were combined (Fig. 1B and C) to form a surface by a skinning algorithm (Jeong et al., 1999). Similarly, the contour lines of the fruit slices on the X-ray CT scans were processed and the shape of the pear was reconstructed. Subsequently, the geometry of the cavity was incorporated in that of the pear, based on the X-ray CT scans. However, due to the spatial limitations of the X-ray CT imaging system, it was not possible to determine the outer contour lines of the whole pear. The CT scans cover only about four-fifths of the pear, since the stem end of the pear could not be measured. Therefore, the cavity needed to be included in the geometrical model of an intact pear based on images taken with the computer vision system as described previously. Hereto, the outer surface fragment from the X-ray CT scans and the geometrical model from the imaging system were matched using a limited set of Euclidean transformations (scaling and translation). The rotation of the surfaces was not necessary because the orientation of the pear was controlled during the X-ray CT and the conventional imaging process. During the X-ray CT imaging, the pear was vertically positioned in front of the detector and this position was marked on the pear surface. Furthermore, the front side of the pear was also marked. The same positioning was used for the conventional imaging. The optimal fit was checked graphically on the computer screen. The transformation values for the outer surface were recorded and the same values were used to calculate the accurate position of the hole. The geometry (Fig. 1D) of the two surfaces (the outer from the three-dimensional modelling system and the cavity from the X-ray CT scans) was transferred to the ANSYS finite element package by means of an automatically generated command script (Jancsó et al., 1997). The script created the two volumes and the final geometry was established by means of the solid modelling capability of the ANSYS program (ANSYS, Inc., USA).

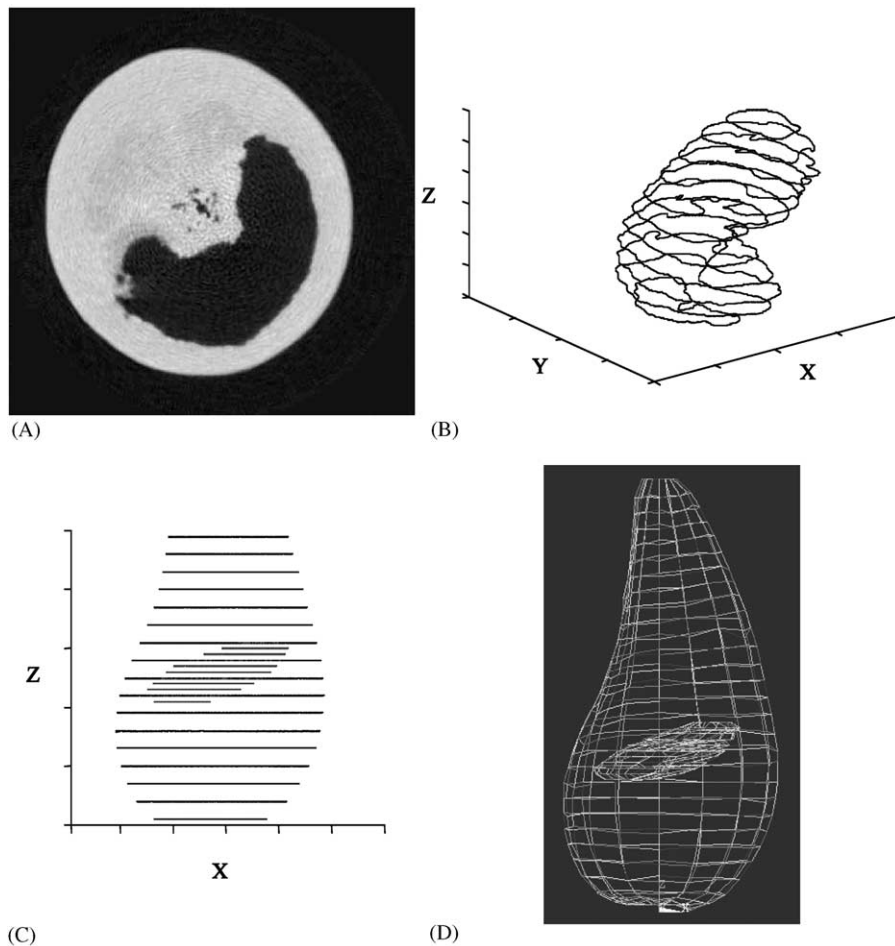


Fig. 1. X-ray CT scan of a pear with a cavity (A). Three-dimensional reconstruction of a pear cavity based on X-ray CT scans. The contours of the cavity are determined for each X-ray CT scan and positioned on top of each other (B), the cavity is positioned in the intact pear (C). Wireframe of intact pear with cavity constructed with image processing system (D).

### 3. Results

#### 3.1. Simulations

##### 3.1.1. Effect of temperature on gas concentration profiles

Table 1 gives an overview of the storage conditions for which respiration–diffusion model simulations were carried out. The effect of temperature on the gas concentration profiles is illustrated in Fig. 2 (left column). Simulations were carried out for a pear stored in air at 20, 7 and  $-1^{\circ}\text{C}$ . The  $\text{O}_2$  gradient over the skin increases with increasing storage temperature. As

temperature increases, the  $\text{O}_2$  consumption increases rapidly and the consumed  $\text{O}_2$  cannot be supplemented sufficiently fast because of diffusion limitations, resulting in decreasing internal  $\text{O}_2$  concentrations. For the same reason, the  $\text{O}_2$  gradient between the centre of the fruit and the boundary increases with temperature. For a pear stored at  $20^{\circ}\text{C}$  in air, the  $\text{O}_2$  concentration in the fruit centre is close to zero. The fermentative metabolism then increases, resulting in extra  $\text{CO}_2$  production. For the pears stored in air at 7 and  $-1^{\circ}\text{C}$ ,  $\text{O}_2$  gradients up to 7 and 3%, between the fruit centre and the storage environment are observed, respectively (Fig. 2).



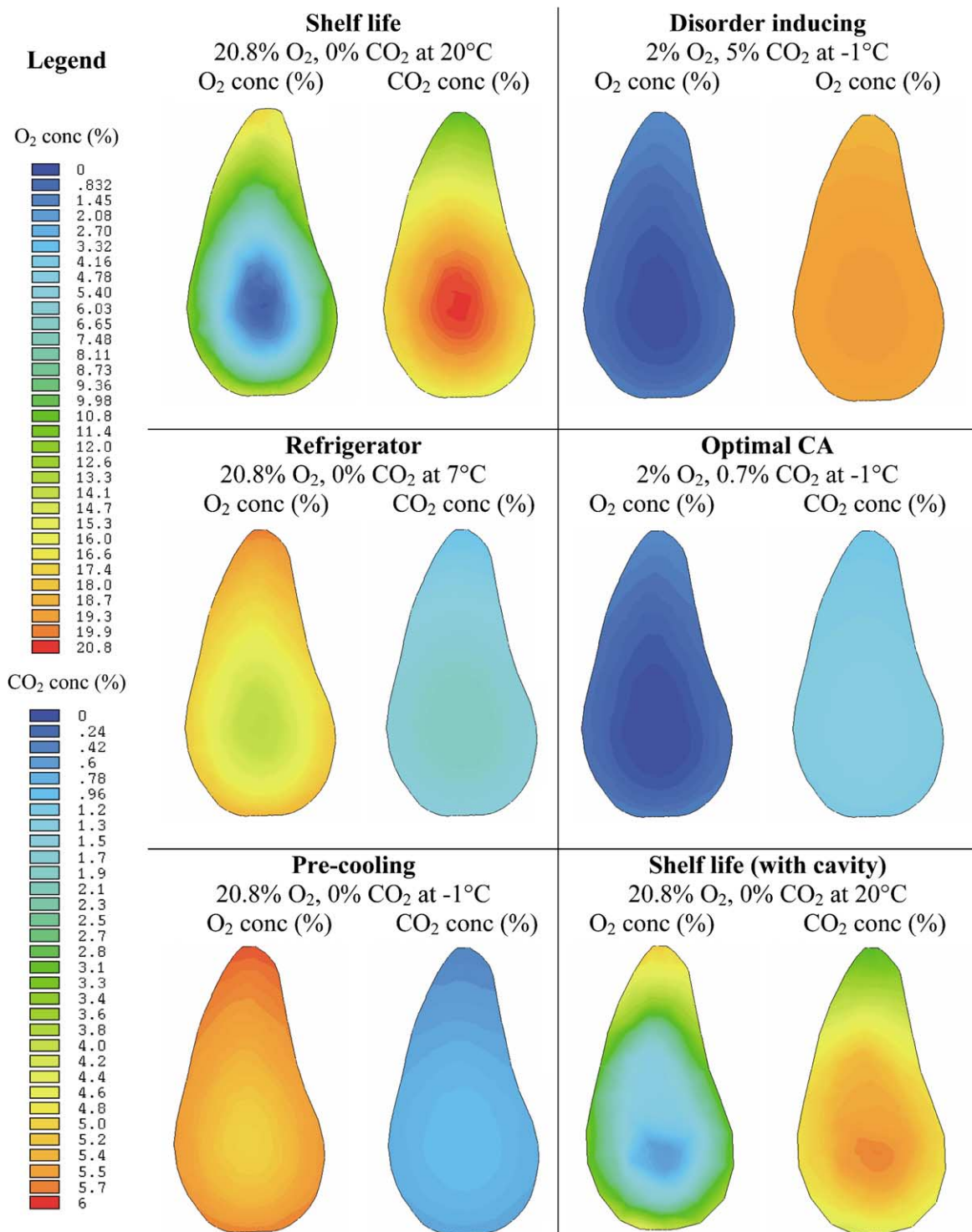


Fig. 2

Similar conclusions can be drawn for CO<sub>2</sub>. Higher storage temperatures increase the CO<sub>2</sub> gradient over the skin and between the centre and the boundary of the fruit. However, since the CO<sub>2</sub> diffusivity and mass transfer coefficient at the skin are higher than for O<sub>2</sub>, the internal gradients and the gradients over the skin are somewhat lower than for O<sub>2</sub>.

### 3.1.2. Effect of storage atmosphere on gas concentration profiles

To study the effect of the storage atmosphere on the steady-state gas concentration profiles, simulations were carried out for a pear cooled at  $-1^{\circ}\text{C}$  in air (20.8% O<sub>2</sub> and 0% CO<sub>2</sub>, Fig. 2) as during delayed controlled atmosphere (DCA) treatment (Lammertyn et al., 2000), a pear stored under disorder-inducing conditions (2% O<sub>2</sub> and 5% CO<sub>2</sub> at  $-1^{\circ}\text{C}$ , Fig. 2) and a pear stored under recommended optimal CA storage conditions (2% O<sub>2</sub> and 0.7% CO<sub>2</sub> at  $-1^{\circ}\text{C}$ , Fig. 2). At  $-1^{\circ}\text{C}$ , the O<sub>2</sub> consumption and CO<sub>2</sub> production rates are very low for all three storage conditions and the gas gradients are very small. The pear stored in air at  $-1^{\circ}\text{C}$  shows a slightly higher O<sub>2</sub> gradient between the fruit centre and the boundary compared to the pears stored at the CA or disorder-inducing condition because of its higher respiration rate. The effect of the ambient CO<sub>2</sub> concentration (0.7 or 5%) on the O<sub>2</sub> concentration is illustrated in Fig. 2. The O<sub>2</sub> concentrations are slightly higher for the pear stored at 5% CO<sub>2</sub> because of the inhibitory effect of CO<sub>2</sub> on the O<sub>2</sub> consumption. However, the differences are small and have the same order of magnitude as the inaccuracy of the numerical solution of the respiration–diffusion model equations. All three CO<sub>2</sub> concentration profiles are quite homogeneous because of the very low respiration rate at  $-1^{\circ}\text{C}$ . At low temperatures, the produced CO<sub>2</sub> diffuses easily towards the fruit skin where it is exchanged with the external atmosphere. As can be expected,

the internal CO<sub>2</sub> concentration in the pear stored under disorder-inducing conditions (5% CO<sub>2</sub>) is higher than that for the pear stored at a low CO<sub>2</sub> concentration (0.7% CO<sub>2</sub>).

### 3.1.3. Effect of a cavity on gas concentration profiles

The effect of the presence of a cavity on the gas concentration profiles is simulated in Fig. 2. The O<sub>2</sub> and CO<sub>2</sub> concentration profiles for a pear without and with a cavity are simulated for shelf-life conditions (air at  $20^{\circ}\text{C}$ ). The cavity is located in the centre of the fruit and clearly influences both gas profiles in the pear. The O<sub>2</sub> and CO<sub>2</sub> concentrations are, respectively, higher and lower in the centre of the fruit, when the cavity is present. Also the gas gradients in the fruit tissue are lower in the presence of a cavity, because of the buffering effect of the cavity.

## 3.2. Sensitivity analysis

### 3.2.1. Gas exchange of the pear with the ambient atmosphere

A sensitivity analysis was performed on the O<sub>2</sub> consumption and CO<sub>2</sub> production rates (or fluxes), simulated with the respiration–diffusion model. The relative sensitivity of the O<sub>2</sub> and CO<sub>2</sub> flux was calculated for every model parameter and this was repeated for three different storage gas atmospheres as indicated in Table 2. Relative sensitivities can be compared between the different parameters. A high absolute sensitivity for a parameter indicates that the model solution is highly influenced by a small change in that parameter value. For shelf-life conditions (20.8% O<sub>2</sub>, 0% CO<sub>2</sub> and  $20^{\circ}\text{C}$ ), the O<sub>2</sub> consumption and CO<sub>2</sub> production rate are both very sensitive to the value of  $V_{m,O_2,cell}$ . As can be expected,  $RQ_{cell}$  has a high influence on the CO<sub>2</sub> production rate but not on the O<sub>2</sub> consumption rate. The parameters involved in the fermentative metabolism are not

Fig. 2. Simulated steady-state O<sub>2</sub> and CO<sub>2</sub> concentration (%) contour plots of pears stored at shelf-life conditions (20.8% O<sub>2</sub>, 0% CO<sub>2</sub> at  $20^{\circ}\text{C}$ ), refrigerator conditions (20.8% O<sub>2</sub>, 0% CO<sub>2</sub> at  $7^{\circ}\text{C}$ ), pre-cooling conditions (20.8% O<sub>2</sub>, 0% CO<sub>2</sub> at  $-1^{\circ}\text{C}$ ), disorder-inducing conditions (2% O<sub>2</sub>, 5% CO<sub>2</sub> at  $-1^{\circ}\text{C}$ ) and optimal CA conditions (2% O<sub>2</sub>, 0.7% CO<sub>2</sub> at  $-1^{\circ}\text{C}$ ). The effect of an internal cavity in a pear, stored at 20.8% O<sub>2</sub>, 0% CO<sub>2</sub> and  $20^{\circ}\text{C}$ , on the O<sub>2</sub> and CO<sub>2</sub> gas concentration contours is also illustrated.

Table 2

Relative sensitivities of O<sub>2</sub> consumption and CO<sub>2</sub> production rates of intact pears with respect to the respiration–diffusion model parameters

| $P_i$   | Ambient atmosphere   |                                     |  |                                     |   |                                     |
|---|--|-------------------------------------|--|-------------------------------------|---|-------------------------------------|
|   | O <sub>2</sub> = 20.8%, CO <sub>2</sub> = 0%, $T = 20\text{ }^{\circ}\text{C}$ |                                     | O <sub>2</sub> = 8%, CO <sub>2</sub> = 15%, $T = 20\text{ }^{\circ}\text{C}$ |                                     | O <sub>2</sub> = 1%, CO <sub>2</sub> = 0%, $T = 20\text{ }^{\circ}\text{C}$ |                                     |
|   | $\bar{J}_{\text{O}_2\text{f},P_i}$   | $\bar{J}_{\text{CO}_2\text{f},P_i}$ | $\bar{J}_{\text{O}_2\text{f},P_i}$   | $\bar{J}_{\text{CO}_2\text{f},P_i}$ | $\bar{J}_{\text{O}_2\text{f},P_i}$  | $\bar{J}_{\text{CO}_2\text{f},P_i}$ |
| $D_{\text{O}_2}$                                | 0.081  | 0.080                               | 0.23   | 0.13                                | 0.030   | −0.18                               |
| $D_{\text{CO}_2}$                               | 0.0093   | 0.0094                              | 0.0013   | 0.0021                              | $-3.9 \times 10^{-5}$   | 0.0017                              |
| $h_{\text{O}_2}$                                | 0.045  | 0.045                               | 0.24   | 0.18                                | 0.84  | 0.062                               |
| $h_{\text{CO}_2}$                               | 0.088  | 0.088                               | 0.026  | 0.032                               | 0.0070  | 0.023                               |
| $V_{\text{m},\text{O}_2,\text{cell}}$           | 0.78   | 0.78                                | 0.52   | 0.62                                | 0.13  | 0.43                                |
| $K_{\text{m},\text{O}_2,\text{cell}}$           | −0.014   | −0.015                              | −0.031   | −0.077                              | −0.70   | −0.32                               |
| $K_{\text{mn},\text{CO}_2,\text{cell}}$         | 0.097  | 0.097                               | 0.17   | 0.21                                | 0.0070  | 0.025                               |
| $V_{\text{m},\text{f},\text{CO}_2,\text{cell}}$ | 0.00   | $1.1 \times 10^{-4}$                | $-8.9 \times 10^{-4}$  | 0.031                               | −0.0047   | 0.66                                |
| $K_{\text{m},\text{f},\text{O}_2,\text{cell}}$  | $-1.3 \times 10^{-5}$  | $1.1 \times 10^{-4}$                | $-4.1 \times 10^{-4}$  | 0.014                               | −0.001  | 0.14                                |
| $\text{RQ}_{\text{cell}}$                       | −0.10  | 0.90                                | −0.027   | 0.94                                | −0.0023   | 0.32                                |

The values of the model parameters are given in Lammertyn et al. (in pressb, Table 1). The index ‘f’ stands for flux. A high absolute sensitivity for a parameter indicates that the model solution is highly influenced by a small change in that parameter value.

addressed at this external gas atmosphere, and hence their relative sensitivity is very low. All model parameters describing gas transport have a low positive sensitivity, referring to an increased respiratory gas flux for higher values of these parameters.

When the pear is stored under 8% O<sub>2</sub> and 15% CO<sub>2</sub> at 20 °C, again a high relative sensitivity is obtained for  $V_{\text{m},\text{O}_2,\text{cell}}$  (both for the O<sub>2</sub> and CO<sub>2</sub> flux) and for  $\text{RQ}_{\text{cell}}$  (for CO<sub>2</sub> flux). Because of the high external CO<sub>2</sub> concentration, the sensitivity of  $K_{\text{mn},\text{CO}_2,\text{cell}}$  on O<sub>2</sub> consumption and CO<sub>2</sub> production increases compared to the aforementioned results for the shelf life conditions. Also the O<sub>2</sub> gas transport parameters ( $D_{\text{O}_2}$  and  $h_{\text{O}_2}$ ) influence the value of both gas fluxes.

For very low O<sub>2</sub> concentrations (1%) and in the absence of CO<sub>2</sub> at 20 °C other parameters exert a high influence on the respiratory gas fluxes. The O<sub>2</sub> flux then becomes very sensitive to  $h_{\text{O}_2}$  and  $K_{\text{m},\text{O}_2,\text{cell}}$  and to a lesser extent to  $V_{\text{m},\text{O}_2,\text{cell}}$ . The CO<sub>2</sub> flux depends strongly on the fermentative parameters ( $V_{\text{m},\text{f},\text{CO}_2,\text{cell}}$  and  $K_{\text{m},\text{f},\text{O}_2,\text{cell}}$ ), but also on the  $V_{\text{m},\text{O}_2,\text{cell}}$  and  $K_{\text{m},\text{O}_2,\text{cell}}$ . A few general conclusions can be drawn from the sensitivity analysis presented in Table 2. First, the sensitivity of the O<sub>2</sub> flux with respect to  $h_{\text{O}_2}$  increases with decreasing O<sub>2</sub> concentration. This parameter de-

termines the O<sub>2</sub> mass transfer through and the O<sub>2</sub> concentration under the skin. Since for low O<sub>2</sub> concentrations the Michaelis-Menten kinetics is very steep, a high sensitivity of  $h_{\text{O}_2}$  on the O<sub>2</sub> flux is to be expected. Second, the influence of  $V_{\text{m},\text{O}_2,\text{cell}}$  on the O<sub>2</sub> flux decreases with O<sub>2</sub> concentration, while the  $K_{\text{m},\text{O}_2,\text{cell}}$  parameter shows the opposite trend. Again this can be explained by the typical shape of the Michaelis-Menten kinetics. Finally, the fermentative parameters ( $K_{\text{m},\text{f},\text{O}_2,\text{cell}}$  and  $V_{\text{m},\text{f},\text{CO}_2,\text{cell}}$ ) show an increasing sensitivity on the CO<sub>2</sub> flux for decreasing O<sub>2</sub> concentrations. For low O<sub>2</sub> concentrations, the fermentative metabolism is increased and the oxidative respiration is slowed down.

### 3.2.2. Gas concentration under the skin

The relative sensitivities for the simulated gas concentrations under the skin are listed in Table 3. At shelf-life conditions, the O<sub>2</sub> concentration is mainly influenced by  $V_{\text{m},\text{O}_2,\text{cell}}$  and  $h_{\text{O}_2,\text{cell}}$ . When  $h_{\text{O}_2,\text{cell}}$  increases at shelf-life conditions, the O<sub>2</sub> concentration under the skin will also increase. Similarly, the CO<sub>2</sub> concentration under the skin is very sensitive to the CO<sub>2</sub> transfer coefficient,  $h_{\text{CO}_2}$ . A decreasing  $h_{\text{CO}_2}$  results in an accumulation of CO<sub>2</sub> under the skin. Also increased  $V_{\text{m},\text{O}_2,\text{cell}}$  and  $\text{RQ}_{\text{cell}}$  favour CO<sub>2</sub> accumulation under the skin.



Table 3

Sensitivity analysis of the respiration–diffusion model simulations of the O<sub>2</sub> and CO<sub>2</sub> concentration under the skin

| $P_i$  | Ambient atmosphere   |                              |   |                              |   |                              |
|--|--|------------------------------|---|------------------------------|---|------------------------------|
|  | O <sub>2</sub> = 20.8%, CO <sub>2</sub> = 0%, $T = 20\text{ }^{\circ}\text{C}$ |                              | O <sub>2</sub> = 20.8%, CO <sub>2</sub> = 0%, $T = 1\text{ }^{\circ}\text{C}$ |                              | O <sub>2</sub> = 0%, CO <sub>2</sub> = 0%, $T = 20\text{ }^{\circ}\text{C}$ |                              |
|  | $\bar{J}_{\text{O}_2, P_i}$  | $\bar{J}_{\text{CO}_2, P_i}$ | $\bar{J}_{\text{O}_2, P_i}$   | $\bar{J}_{\text{CO}_2, P_i}$ | $\bar{J}_{\text{O}_2, P_i}$   | $\bar{J}_{\text{CO}_2, P_i}$ |
| $D_{\text{O}_2}$                                   | −0.058   | 0.093                        | −0.0019   | 0.0004                       | —   | —                            |
| $D_{\text{CO}_2}$                                  | −0.005   | 0.003                        | −0.0002   | −0.0055                      | —   | −0.009                       |
| $h_{\text{O}_2}$                                   | 0.436  | 0.051                        | 0.0656  | 0.0004                       | —   | —                            |
| $h_{\text{CO}_2}$                                  | −0.038   | −0.906                       | −0.0015   | −0.9674                      | —   | −0.991                       |
| $V_{\text{m}, \text{O}_2, \text{cell}}$            | −0.335   | 0.759                        | −0.0619   | 0.9719                       | —   | —                            |
| $K_{\text{m}, \text{O}_2, \text{cell}}$            | 0.007  | −0.015                       | 0.0004  | −0.0063                      | —   | —                            |
| $K_{\text{mn}, \text{CO}_2, \text{cell}}$          | −0.043   | 0.097                        | −0.0017   | 0.0272                       | —   | —                            |
| $V_{\text{m}, \text{f}, \text{CO}_2, \text{cell}}$ | 0.00   | 0.00                         | 0.00  | 0.0003                       | —   | 1                            |
| $K_{\text{m}, \text{f}, \text{O}_2, \text{cell}}$  | 0.00   | 0.00                         | 0.00  | 0.00                         | —   | —                            |
| $\text{RQ}_{\text{cell}}$                          | 0.043  | 0.903                        | 0.0017  | 0.9728                       | —   | —                            |

The values of the model parameters are given in Lammertyn et al. (in pressb, Table 1). A high absolute sensitivity for a parameter indicates that the model solution is highly influenced by a small change in that parameter value. Irrelevant sensitivities are denoted by an ‘—’.

When the temperature is decreased to 1 °C, the sensitivity of O<sub>2</sub> towards  $V_{\text{m}, \text{O}_2, \text{cell}}$  and  $h_{\text{O}_2}$  decreases. However, the effect of  $h_{\text{CO}_2}$ ,  $\text{RQ}_{\text{cell}}$  and  $V_{\text{m}, \text{O}_2, \text{cell}}$  on the CO<sub>2</sub> concentration grows with decreasing temperature. For pears stored in a N<sub>2</sub> atmosphere, a sensitivity analysis can only be carried out for CO<sub>2</sub> as a function of three model parameters only, since all the other parameters vanish from the model. The CO<sub>2</sub> concentration is very sensitive to  $V_{\text{m}, \text{f}, \text{CO}_2, \text{cell}}$  and  $h_{\text{CO}_2}$ .

### 3.3. Respiration–diffusion model in relation to core breakdown

Pears were stored under disorder-inducing conditions to develop cavities. After 9 months, three pears with the largest cavities were selected and stored at the atmospheres indicated in Table 4. The gas concentration in the cavity was measured by GC and compared to the one simulated with the respiration–diffusion model. The respiration–diffusion model was applied for simulations on a pear geometry including a cavity. The results are summarised in Table 4. For the pear stored in a N<sub>2</sub> atmosphere at 20 °C and the one stored in air at 1 °C, the simulated values (indicated by asterisks) show a close agreement with the measured ones, both for the gas concentration in the cavity and

under the skin. For the pear stored in air at 20 °C, good model predictions were made for the skin concentration for both gases. However, the measured O<sub>2</sub> cavity concentration was more than three times higher than the simulated one. This might be explained by different gas diffusion properties of affected tissue. Dried brown tissue has a lower moisture content, more intercellular air spaces and hence the gas diffusion coefficients may be higher for this type of tissue than for healthy tissue, on which the model is based. To test this hypothesis, in a new set of simulations (indicated by +) the O<sub>2</sub> and/or CO<sub>2</sub> diffusion coefficients were increased. Without affecting the gas concentration under the skin, improved model predictions were obtained for the gas concentration in the cavities. The adapted values of the O<sub>2</sub> and CO<sub>2</sub> diffusion coefficients are 10–15 times higher (for O<sub>2</sub>) and two times higher (for CO<sub>2</sub>) than those reported in Lammertyn et al. (2003b) for healthy tissue (Table 4). It should be noted here that the diffusion coefficients determined on these affected pears reflect the joint gas diffusion properties of a system of unaffected and affected tissues. They may also be affected by the diffusion characteristics of the cavity wall. To know the real diffusion characteristics of affected tissue, diffusion-independent diffusion measurements should be carried out for

Table 4

Measured and simulated gas concentrations under the skin and in the cavities of affected pears at three ambient atmospheres

|  | Ambient atmosphere                         |   |   |
|--|--|---|---|
|  | $O_2 = 20.8\%, CO_2 = 0\%, T = 20^\circ C$ | $O_2 = 20.8\%, CO_2 = 0\%, T = 1^\circ C$ | $O_2 = 0\%, CO_2 = 0\%, T = 20^\circ C$ |
| Measured                                     |  |   |   |
| O <sub>2</sub> cavity (%)                    | 14.1                                       | 20.8                                      | 0.4                                     |
| CO <sub>2</sub> cavity (%)                   | 7.9  | 0.6                                       | 2.6                                     |
| O <sub>2</sub> skin (%)                      | 14.7                                       | 20.7                                      | 0.2                                     |
| CO <sub>2</sub> skin (%)                     | 4.8  | 0.6                                       | 4.0                                     |
| Simulated                                    |  |   |   |
| O <sub>2</sub> cavity (%)                    | 13.8 <sup>+</sup> /4.6*                    | 19.7 <sup>+</sup> /18.0*                  | 0.0 <sup>+</sup> /0.0*                  |
| CO <sub>2</sub> cavity (%)                   | 5.5 <sup>+</sup> /5.1*                     | 0.2 <sup>+</sup> /0.3*                    | 3.0 <sup>+</sup> /4.0*                  |
| O <sub>2</sub> skin (%)                      | 14.4 <sup>+</sup> /14.1*                   | 19.8 <sup>+</sup> /19.6*                  | 0.0 <sup>+</sup> /0.0*                  |
| CO <sub>2</sub> skin (%)                     | 4.6 <sup>+</sup> /4.6*                     | 0.1 <sup>+</sup> /0.1*                    | 3.2 <sup>+</sup> /4.1*                  |
| Adapted parameters                           |  |   |   |
| $D_{O_2}$ (m <sup>2</sup> s <sup>-1</sup> )  | $7 \times 10^{-8}$                         | $5 \times 10^{-8}$                        | —                                       |
| $D_{CO_2}$ (m <sup>2</sup> s <sup>-1</sup> ) | —  | —   | $8 \times 10^{-8}$                      |

The values marked with \* indicate the simulated gas concentrations before adaptation of the diffusion parameters, while those denoted by + refer to the simulated values based on the adapted diffusion coefficients. The parameter values are listed in Lammertyn et al. (in pressb, Table 1).

brown tissue. Changes in maximal O<sub>2</sub> consumption and fermentative CO<sub>2</sub> production rates due to tissue browning are not taken into account, since it is not clear whether the cells have an increased respiration due to stress or have a decreased respiration because of cell death. For the pear stored at 1 °C in air, the simulated and measured concentrations under the skin and in the cavity corresponded well, also before the adaptation of the O<sub>2</sub> diffusivity. Since the respiration is very low at 1 °C, almost only diffusion processes will take place. Hence, in steady-state conditions, everywhere in the pear the internal O<sub>2</sub> and CO<sub>2</sub> concentrations will eventually be close to the ambient gas concentrations.

#### 4. Discussion

The respiration–diffusion model allows quick simulations of gas concentration profiles in pears stored at different gas atmospheres and temperatures. Simulations have shown that for pears stored under disorder-inducing conditions (2% O<sub>2</sub> and 5% CO<sub>2</sub> at –1 °C), O<sub>2</sub> concentrations are reached close to or lower than the anaerobic compensation point or with an order of magnitude

of the  $K_{m,O_2,cell}$  value only in the very centre of the fruit. At these low concentrations, respiration and ATP production decrease considerably, resulting in a lower energy level for maintenance reactions such as repairing membrane damage. Hence, membrane damage is only expected at (very low) O<sub>2</sub> concentrations where the demand for ATP exceeds the ATP production. To determine these critical O<sub>2</sub> concentrations, more insight into the cellular ATP demand is necessary. X-ray CT scans and MR images reveal that tissue browning also occurs at positions corresponding to higher O<sub>2</sub> concentrations and thus higher energy levels, where probably no shortage of ATP occurs. No strict relation between steady-state O<sub>2</sub> concentration (or respiration rate) profiles and the location of internal browning (and cavity development) exists. It is also known that vitamin C decreases rapidly in pears stored under CA conditions with an elevated CO<sub>2</sub> level (Veltman et al., 2000). In this respect, vitamin C cannot scavenge O<sub>2</sub> radicals anymore, which now can attack the membranes, resulting in decompartmentation and internal browning. In previous simulation experiments, it has been shown that at low storage temperatures the CO<sub>2</sub> concentration is almost uniformly distributed in the pears and only slightly higher than

the ambient concentration. Hence, no clear relationship seems to exist between the steady-state CO<sub>2</sub> concentration contours and the pattern of browning. Larger gas gradients mainly occur for pears at increased temperatures. Here the respiration rate is much faster than the gas diffusion in the fruit, resulting in considerable gradients. Lammertyn et al. (2000) and Roelofs and de Jager (1997) illustrated that delayed controlled atmosphere has an important effect on the incidence of internal browning. Pears cooled at  $-1^{\circ}\text{C}$  in air for a period of at least 21 days were far less susceptible than those placed immediately under CA conditions. Freshly harvested pears have a temperature around  $20^{\circ}\text{C}$  and, hence, a high respiration rate. When they are stored immediately under commercial CA storage conditions, the ambient atmosphere will change from air to 2% O<sub>2</sub> and 0.7% CO<sub>2</sub> at  $-1^{\circ}\text{C}$ . Depending on the stacking of the bins and the airflow in the cooling room, the cooling down period may last a couple of days to even 1 week or more. In this period, the O<sub>2</sub> concentration will decrease dramatically in the fruit, because the temperature and thus the respiration are still high. More O<sub>2</sub> is consumed inside the pear than can be provided via diffusion from the ambient atmosphere. Large parts of the fruit will now experience an O<sub>2</sub> concentration which might induce membrane damage and internal browning. Locally in the bins the O<sub>2</sub> concentration may be even lower than the indicated O<sub>2</sub> concentration for the CA storage room. At the same time, CO<sub>2</sub> increases in the fruit, affecting the vitamin C and hence the anti-oxidant capacity. When the pears are treated with delayed CA (DCA), they are first cooled down ( $-1^{\circ}\text{C}$ ) in air for a period of at least 3 weeks. Afterwards, when the respiration stress due to harvest has disappeared and the pears are properly cooled down, they are brought under the commercial CA storage conditions. The storage scenarios are reconstructed for O<sub>2</sub> concentration profiles with DCA and immediate application of CA. Without DCA, the O<sub>2</sub> concentration reaches very low levels at which membrane damage might occur (Fig. 3). If this hypothesis holds, it would mean that when fruit are properly cooled before storage under CA conditions, the O<sub>2</sub> and CO<sub>2</sub> concentration set

points during that storage may be chosen lower and higher, respectively, as long as the O<sub>2</sub> concentrations in the fruit do not decrease beyond the critical O<sub>2</sub> concentration at which membrane damage is induced. This would result in higher pear quality retention. The beneficial effect of DCA on the incidence of core breakdown might partially be attributed to the effect of the interaction between temperature and the applied gas atmosphere during the first weeks of storage. However, it does not explain why, for instance, pears stored for 4 weeks under DCA treatment are less susceptible to the disorder than for pears stored for 2 weeks under DCA. Neither does it explain why a DCA treatment of 1 week seems to be the worst scenario (Roelofs and de Jager, 1997). Another unknown beneficial factor might be involved such as the adaptation capacity (e.g. with respect to the membrane lipid composition) of the pear to environmental factors. However, this is purely hypothetical and further research is certainly required to identify or prove the existence of these factors.

Simulations have pointed out that the presence of a cavity influences the gas profile contours of the pear. It has also been shown that the respiration–diffusion model predicts the lowest O<sub>2</sub> and highest CO<sub>2</sub> concentrations in the centre of the fruit, exactly at the position where in non-parthenocarpic pears, the core is located. If now a small cavity, with the dimensions of the core, is positioned in the centre of the fruit, slightly higher O<sub>2</sub> and lower CO<sub>2</sub> concentrations will be obtained in the centre of the pear. Moreover, if this core cavity was connected to the ambient atmosphere via a very small style channel, the O<sub>2</sub> and CO<sub>2</sub> concentrations in the cavity would be higher and lower, respectively, than those of the surrounding tissue. This would then result in gas profiles with a minimum O<sub>2</sub> concentration in the middle between the fruit boundary and the core, and a maximum CO<sub>2</sub> concentration at the same position. This pattern will then be very close to the browning pattern observed on MRI and X-ray CT scans. However, more research needs to be done about the presence and the function in gas exchange of this open style channel.

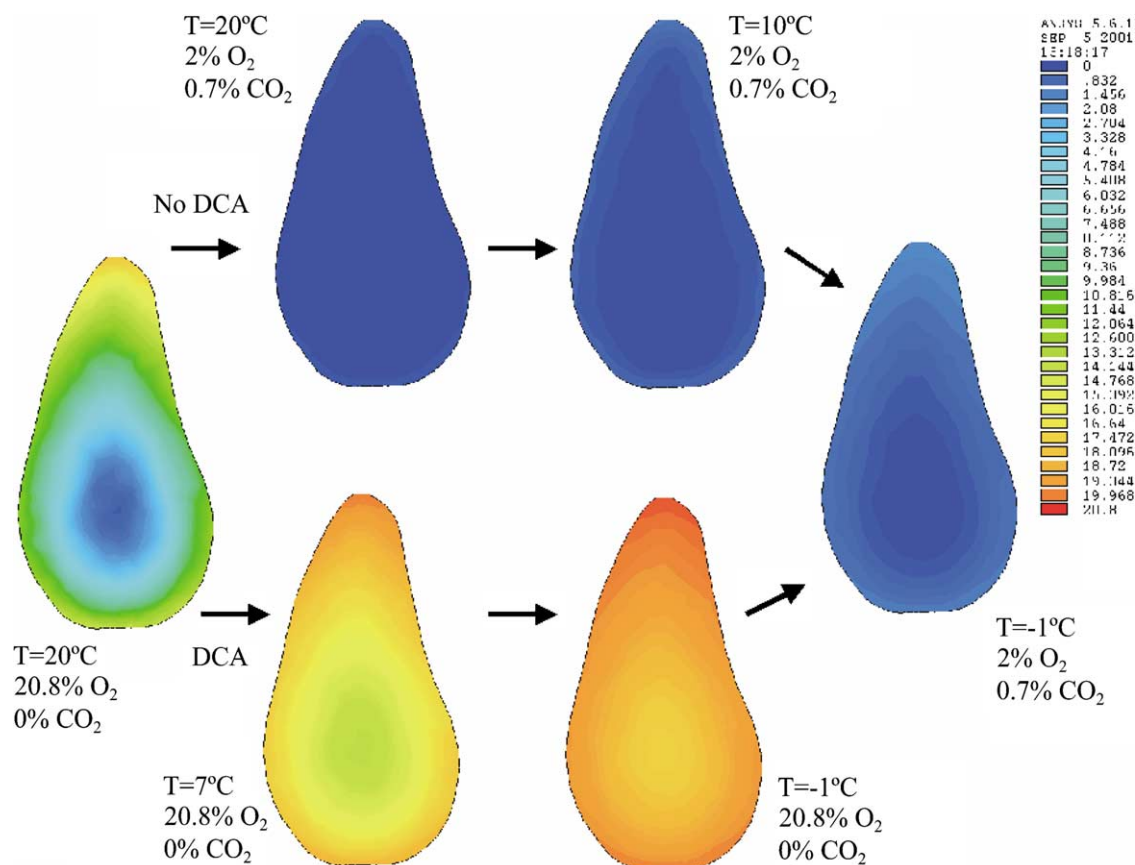


Fig. 3. Oxygen concentration (%) profiles of a pear stored under DCA treatment, or brought immediately under CA conditions. Without DCA, membrane damage might have occurred because of the very low  $\text{O}_2$  concentrations.

## 5. Conclusion

A validated respiration–diffusion model for pears was used to quickly calculate the internal gas concentration profiles of fruits stored under various storage atmospheres and to relate these profiles to core breakdown disorder. It was found that the skin formed the major barrier to gas transport, but that the internal gas gradients could not be neglected. Especially at high temperatures, because of the increased respiration, internal gradients increased considerably. At commercial CA storage conditions, the  $\text{O}_2$  concentrations and gradients in the fruit were low, but not low enough to induce irreversible membrane damage and hence core breakdown. A comparison of the simulated gas concentration contours of pears

treated with delayed controlled atmosphere storage and those of pears immediately stored after harvest in commercial storage conditions, strongly indicated the importance of a good gas atmosphere and temperature management the first month of storage. A sensitivity analysis pointed out that the influence of the parameters on the model simulations depended on the storage atmosphere of the pears. It was found that the gas concentrations under the skin were mainly determined by the surface gas transfer coefficients and the maximal  $\text{O}_2$  consumption rate. The internal gas gradients were sensitive to the values of the gas diffusivities and the fermentative  $\text{CO}_2$  production rate. The validity of the model for affected pears was tested by comparing the gas composition in the cavity of an affected pear with the predicted

gas composition. Based on the latter experiment, it could be suggested that the gas diffusion properties of affected brown discoloured tissue were different from those obtained for healthy tissue. The respiration–diffusion model has proven to be a promising tool to study and simulate the effect of controlled atmosphere conditions on the incidence of core breakdown during storage.

## Acknowledgements

The Belgian Ministry of Small Enterprises, Traders and Agriculture and the Flemish Government are gratefully acknowledged for financial support (project S-5901). This research was also financially supported by the European Union (EC-FAIR1-CT96-1803) and the Catholic University Leuven (IDO-project 00/008). Jeroen Lammertyn is postdoctoral fellow with the Flanders Fund for Scientific Research (FWO-Vlaanderen).

## References

- Abdul-Baki, A.A., Solomos, T., 1994. Diffusivity of carbon dioxide through the skin and flesh of 'Russet Burbank' potato tubers. *J. Am. Soc. Hort. Sci.* 119, 742–746.
- Hertog, M.L.A.T.M., Peppelenbos, H.W., Evelo, R.G., Tijskens, L.M., 1998. A dynamic and generic model on the gas exchange of respiring produce: the effects of oxygen, carbon dioxide and temperature. *Postharvest Biol. Technol.* 14, 335–349.
- Jancsók, P., 1999. Geometrical model generation for finite element meshes of biological products based on digital image processing. Ph.D. Thesis. Faculteit Landbouwkundige en Toegepaste Biologische Wetenschappen, Katholieke Universiteit Leuven.
- Jancsók, P., Nicolaï, B.M., Coucke, P., De Baerdemaeker, J., 1997. 3D finite element model generation of fruits based on image processing. In: Munack, A., Tantau, H. (Eds.), *Mathematical and Control Application in Agriculture and Horticulture*, September 28–October 2, 1997, Hannover, Germany, pp. 131–135.
- Jancsók, P., Clijmans, L., Nicolaï, B.M., De Baerdemaeker, J., 2001. Investigation of the effect of shape on the acoustic response of 'Conference' pears by finite element modelling. *Postharvest Biol. Technol.* 23, 1–12.
- Jeong, J., Kim, K., Park, H., Cho, H., Jung, M., 1999. B-spline surface approximation to cross-sections using distance maps. *Int. J. Adv. Manuf. Technol.* 15, 876–885.
- Lammertyn, J., Aerts, M., Verlinden, B.E., Schotmans, W., Nicolaï, B.M., 2000. Logistic regression analysis of factors influencing core breakdown in 'Conference' pears. *Postharvest Biol. Technol.* 20, 25–37.
- Lammertyn, J., Dresselaers, T., Van Hecke, P., Jancsók, P., Wevers, M., Nicolaï, B.M., 2003a. Analysis of the time course of core breakdown in 'Conference' pears by means of MRI and X-ray CT. *Postharvest Biol. Technol.* 29, 19–28.
- Lammertyn, J., Scheerlinck, N., Jancsók, P., Verlinden, B.E., Nicolaï, B.M., 2003b. A respiration–diffusion model for 'Conference' pears. I. Model development and validation. *Postharvest Biol. Technol.* 30, 29–42.
- Mannapperuma, J.D., Singh, R.P., Montero, M.E., 1991. Simultaneous gas diffusion and chemical reaction in foods stored in modified atmospheres. *J. Food Eng.* 14, 167–183.
- Nicolaï, B.M., Scheerlinck, N., Verboven, P., De Baerdemaeker, J., 2000. Stochastic perturbation analysis of thermal food processes with random field parameters. *Trans. ASAE* 43, 131–138.
- Rabus, C., Streif, J., Bangerth, F., 2001. Simulation model for the calculation of internal gas exchange in apple fruits. *Acta Hort.* 553, 595–597.
- Roelofs, F.P., de Jager, A., 1997. Reduction of Brownheart in 'Conference' pears. In: Mitcham, E. (Ed.), *Proceedings. Vol. 2. Apples and Pears, Controlled Atmosphere Research Conference*, July 13–18, 1997. University of California, Davis, USA, pp. 138–144.
- Veltman, R.H., Kho, R.M., van Schaik, A.C.R., Sanders, M.G., Oosterhaven, J., 2000. Ascorbic acid and tissue browning in pears (*Pyrus communis* L. cvs. Rocha and Conference) under controlled atmosphere conditions. *Postharvest Biol. Technol.* 19, 129–137.
- Wang, C.Y., Wang, P.C., 1989. Nondestructive detection of core breakdown in 'Bartlett' pears with nuclear magnetic resonance imaging. *HortScience* 24, 106–109.
- Yearsley, C.W., Banks, N.H., Ganesh, S., 1997. Effect of carbon dioxide on the internal lower oxygen limits of apple fruit. *Postharvest Biol. Technol.* 12, 1–13.